Mould Design Improvement and Flaw Analysis for Investment Casting Process using Numerical Computation with Experimental Validation

A. R. A. Rahman[1], Y. H. P. Manurung[1, *], K. Kasim[2], M. S. Adenan[1], M. F. Mat[1], Y. O. Busari[1,3], I. Siregar[4], T. C. Kung[5], A. Syafiq[6]

[1]Smart Manufacturing Research Institute (SMRI), School of Mechanical Engineering, College of Engineering, UiTM Shah Alam, Selangor, Malaysia.
[2]Department of Mechanical Engineering, Politeknik Sultan Salahuddin Abdul Aziz Shah, Shah Alam, Selangor, Malaysia.
[3]Department of Materials & Metallurgical Engineering, University of Ilorin, PMB1515, Nigeria
[4]Department of Industrial Engineering, Universitas Sumatera Utara, Malaysia
[5]Sales & Marketing Manager, Fetta Lost Wax Casting, Bukit Rambai, Malacca, Malaysia.
[6]Production Solution Manager, ORS Technologies Sdn Bhd, W.P Kuala Lumpur, Malaysia.

ABSTRACT: Investment casting is recognized for producing intricate shapes in a single process, eliminating the need for multiple manufacturing and assembly processes for welding and bending. However, challenges remain where flaws, such as shrinkage porosity can affect product quality. This research uses numerical simulations using Altair Inspire Cast to minimize flaws in the investment casting process for vehicle barrier support components made from stainless steel 304. This study begins with a numerical simulation of an existing mould design based on actual process parameters, followed by an experimental investigation of flaw occurrence and location. Several casting designs were tested, analysing liquid metal behaviour during filling and solidification. The initial design of Case 1a showed 455 mm³ of shrinkage volume, which was eliminated by rotating the casting parts 90 degrees in Case 1b. A further design improvement in Case 2a increased the casting yield by over 10% by reducing 50% the gating system height. However, without optimal parameters, cold shuts were introduced. Case 2b, which uses a shorter filling time of 10 seconds successfully mitigates the cold shut. Final design modifications (Case 3) were validated through actual fabrication, showing that flaw location could be predicted and process optimization achieved for higher-quality products.

KEYWORDS: Altair Inspire Cast; Cold shut; Investment casting; Optimization; Shrinkage porosity

[Received Sep. 15, 2024; Revised Feb. 18, 2025; Accepted Feb. 26, 2025] Print ISSN: 0189-9546 | Online ISSN: 2437-2110

I. INTRODUCTION

Investment casting, commonly called lost wax casting, goes back to 4000 BCE. The investment casting procedure is prominent today because intricacy and thin-wall components are necessary for critical sectors like automotive and aerospace (Jones et al., 2020). Moreover, dimensional perfection and lowered prerequisites for post-treatment may increase castability for a fraction of the initial cost. Investment casting avoids mismatch flaws compared to other casting processes with the same gravity pouring since just one mould is required for the investment casting method. Unfortunately, undesirable outcomes or flaws might occur in the casting component throughout metal casting production. Cold shuts, shrinkage porosity, gas porosity, non-fill, distortion, and cracking are typical flaws in casting manufacturing, particularly when the investment casting method is used (Rafique and Iqbal, 2009).

Many decades ago, the development of the investment casting process relied heavily on trial and error to ascertain the optimal flaw-free casting process, parameter, and runner design while enhancing casting yield. Technical expertise and skill are essential in product development and are frequently associated with a long track record of craftsmanship. Nevertheless, the process seems more time-consuming when the market necessitates a quick product redesign (Malik et al., 2020)

Hence, worldwide industrial manufacturing process are transforming product development paradigm towards a greater focus on scientific simulation (Ahmad et al., 2022; Choe et al., 2022). The computer-aided engineering may represent the complete casting process and visualize the filling and solidification of molten metal under actual working circumstances using proper and sufficient parameters. In addition, the fundamental cause of flaws, such as shrinkage porosity, cold shuts, and misrun, may be recognized in the early stages of preliminary casting design, preventing expensive production corrections or waste.

The correlation between the actual casting process, simulation setup, modelled physical attributes, governing equation, and variables are essential components of the computational model to understand the underlying casting process (Fu & Yong, 2009). Reliable and realistic parameter

*Corresponding author: yupiter.manurung@uitm.edu.my
doi http://dx.doi.org/10.4314/njtd.v22i1.2910

input for the cast component and shell mould is required to simulate the actual casting process. Little variations in the metal composition and parameters may affect particular characteristics of the metal behaviour, especially in austenitic stainless steel (Khan and Sheikh, 2018; Mat et al., 2020). Consequently, the software needs to facilitate the modification of all casting material parameters in optimizing the casting process, which replaces the traditional interactive trial-and-error technique with a virtual approach. With this method, designers can access various possible designs that may be used to refine the casting process.

The filling time is an essential stage for the investment casting process because the filling time interval can impact the casting soundness and quality of the final cast, particularly for big thin-wall castings in which filling-related flaws such as misrun and cold shut are more common. A turbulent flow that results from a filling time that is too quick might lead to porosity flaws and oxidation inclusions. Thus, throughout the filling process, an appropriate filling time is necessary B. Sun et. al. (2021). The investment casting of the K424 alloy thin-wall filling process was investigated in (X. Wang and Zhang, 2011). It was discovered that even if the pouring temperature is high, low shell temperature can cause the pouring temperature to drop quickly during the contact with the sprue by 100 °C, and from the sprue to within the casting, it falls by 200 °C. The poured metal can solidify prematurely before the process is complete if the temperature is close to the solidus temperature of 1237 °C.

The sequencing of the filling process will result in the occurrence of a cold shut and misrun. When two front metals become partially solid and partially liquid during the confluence of liquid metal, the low temperature may result in cold shuts because the confluence cannot fully fuse the two front metals. Based on the volume of fluid (VOD) algorithm studied by Feng et. al. (2021), the nature of liquid metal flow during the casting process was determined. The calculations' findings provide an outcome that is consistent with the experiment. The cold shut event may be easily formed outside of the flow path. Moreover, it can also occur within a distance from the runner and in a thin wall. The cold shut may impact the casting components' mechanical qualities and surface dimensions. If insufficient molten metal is used in the casting process, there will be tiny holes throughout the casting process when the metal cools and contracts during the solidification step. The final isolated region of the freezing zone is often where shrinkage porosity is most prone to occur (Bruna et al., 2019). Shrinkage porosity may degrade the casting quality and weaken the components' structural integrity.

Previous research has shown that casting flaws are due to improper gating location (Šabík et al., 2021). To compensate for metal shrinkage that occurs during the solidification stage of the investment casting process, the assembly of the gating system is essential. The investment casting's gating structure comprises the pouring cup, runner, gate, and air vent. Runners are attached to the casting assembly at an appropriate spot to confine the shrinkage porosity, which is the flaw in secondary components that will be eliminated during the cutting process Kumar et. al. (2018); Kuo et. al. (2017). Because of the intricate shape of the hydraulic retarder impeller and thin edge, improving the gating system can help eliminate the flaws linked to the filling and solidification process. Previous study shows that one of the three casting designs used in the simulation program can give the impeller a sufficient filling and solidification process, which is the case with only one extension of the gating system. The experiment serves to validate the successful conclusion reached by the simulation. The x-ray findings on the actual component reveal no flaws in the impeller, which complements the simulation results for the investment casting of the impeller (Li et al., 2021).

A larger gating layout is the most straightforward method for foundries to prevent solidification-related flaws. Under mass-scale production, the technique caused many scrapped metals, resulting in lower casting yield. The cost to remelt discarded metal added to the overall manufacturing cost (Carlson et al., 2002). The optimized casting design helps the foundry lower costs and improve profitability without neglecting the casting flaws.

This study aims to investigates an industrial case study of the investment casting process over its casting product rejection due to the occurrence of flaws. Figure 1 shows the industrial casting flaws and shrinkage porosity that occurred in the preliminary casting design of the austenitic stainless steel SS304 casting part, which is the vehicle barrier support. By utilizing the numerical simulation with experimental validation, the study aims to provide a comprehensive methodology for predicting and mitigating casting flaws leading to higher-quality products and manufacturing efficiency.

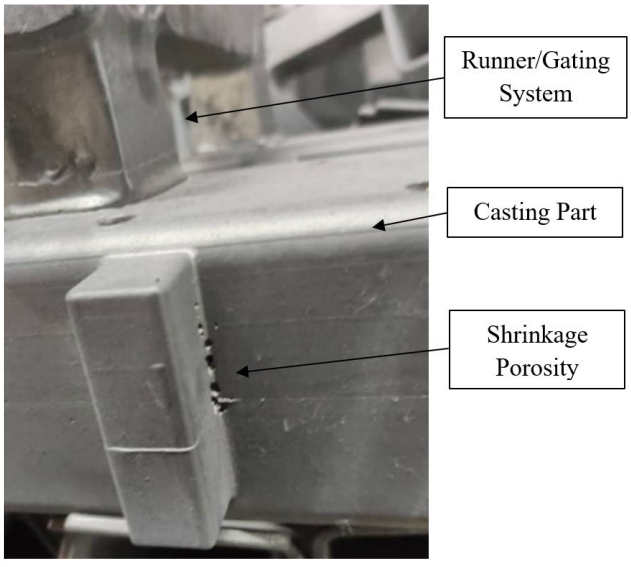

Figure 1: The porosity at the fabricated part (vehicle barrier support)

II. METHODS AND PROCEDURE

A framework of the investment casting process used in this study is represented in Figure 2. The casting design, consisting of the gating system, is closely related to the geometry of the casting parts' product design. The stream of molten metal from the runner to the shell cavity of the casting

part contributed to the occurrence of flaws. Considering the casting process's design, material properties, and parameters, the simulation results provide information about the filling and solidification of the molten metal. Based on the identified factors that cause the flaws, the new optimized casting system is re-simulated to obtain permissible or flaws-free casting for production.

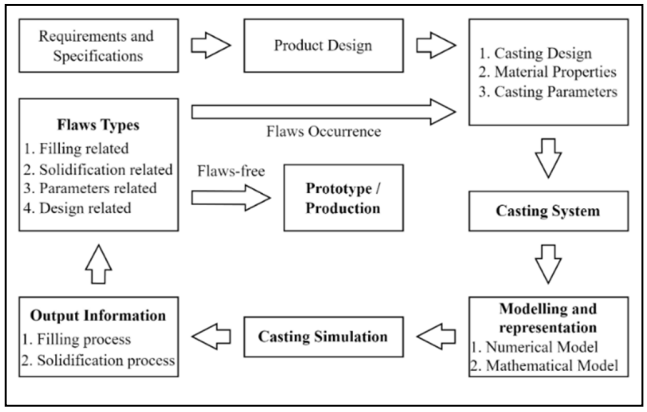

Figure 2: The casting simulation procedure for identifying flaws

A. Experimental Setup

A preliminary experiment, case 1a of the investment casting process was conducted to evaluate the application of the numerical casting simulation. Figure 3 shows the investment casting process begins by making a wax pattern of vehicle barrier support to be cast. Two wax patterns of vehicle barrier support were assembled to the runner and attached to the pouring cup. The patterns, runners, and pouring cups formed the tree of the shell mould. This tree is further dipped in the refractory's zircon slurry bath and later to be drained off. The wet layer is immediately stuccoed with fine zircon sand to form the first layer of the shell. The first coating of the shell is allowed to dry in the temperature control room for several hours. These steps are repeated until the seven layers are stuccoed with coarse zircon sand. Later, the hardened shell is dewaxed in the autoclave to remove the wax and preheated to a superheated temperature to eradicate the residual wax and to withstand thermal shock during pouring. The material SS304 was melted in the induction furnace which later was gravity poured into the zircon shell mould. Upon completing the investment casting process, hammering knocked the shell mold off to remove the shell from the casting part. The casting part was cut off from the tree using a sawing machine. The visual inspection was conducted to adhere to the visual acceptance standards and identify surface flaws.

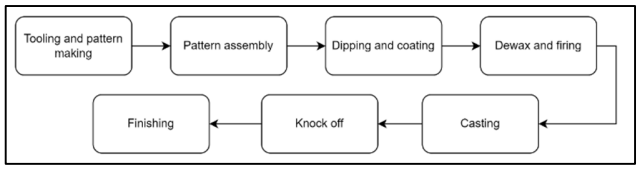

Figure 3: The flowchart of the whole investment casting process

B. Numerical Simulation Setup and Procedure

The significant parameters of the experimental investment casting process are measured to establish a meaningful comparison later in numerical casting simulation. This research uses Altair Inspire Cast 2021 (formerly Click2Cast) to evaluate the virtual casting procedure to quality standards comprehensively. The software deliberates on speeding up manufacturing high-quality cast components with a highly intuitive user interface design for academic and professional purposes. Recurring flaws such as porosity, cold shuts, air entrapment, and distortion can be evaluated and visualized using Inspire Cast as early as the design process. The software is capable of simulating Low-Pressure Die Casting (LPDC), High-Pressure Die Casting (HPDC), Gravity Casting, Gravity Tilt Pouring, and Investment Casting (Jadhav and Mane, 2020).

1) Geometrical model and material properties

Figure 4 illustrates the drawing configuration of the foundry's vehicle barrier support. Based on the sketch, the computer-aided design (CAD) model is developed using CATIA V5R21, a commercial CAD program. Each side has four holes with a radius of 4.25 mm and one with a radius of 6.10 mm. The minimum thickness of the vehicle barrier support is 5 mm, and the maximum length is 250 mm. The CAD model of the vehicle barrier support is then exported in STL format to Altair Inspire Cast.

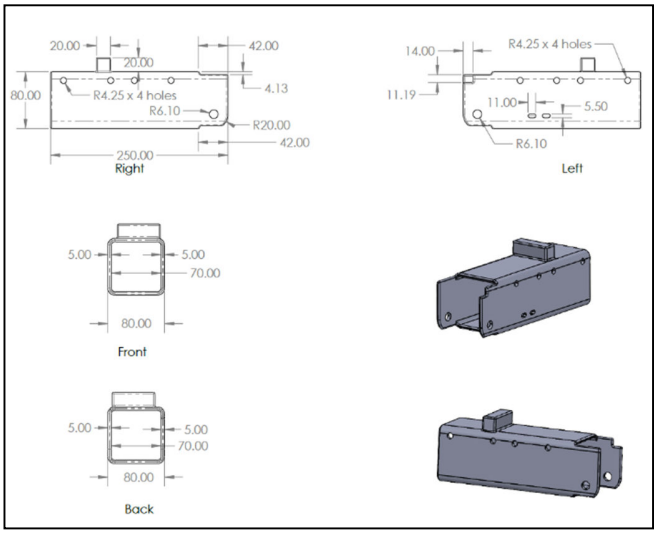

Figure 4: Technical drawing of the casting product

The SS304 is renowned for its exceptional thermal properties. As it can withstand high temperatures without deteriorating, it is an ideal material for high-temperature processing equipment, heat exchangers, boilers, and other applications that need high-temperature usage.

The high Chromium (Cr) and Nickel (Ni) composition provides good corrosion resistance and durability (Liu et al., 2022). The predominant austenite crystal structure prevents the steel from being hardened by heat treatment. The composition of SS304 is shown in Table 1 (D. Wang et al., 2018). The thermophysical and thermal properties of the material calculated by Altair Inspire Cast are provided in Tables 3 and

Figure 4. Knowing the thermophysical properties of the material used in the simulation is essential because these properties determine how the fluid flows and solidifies. The simulation model's accuracy in comparing the material's actual behaviour significantly depends on the selection of the thermophysical properties.

It can be observed that there are considerable variations in the thermal conductivity value of the SS304. High temperatures increase thermal conductivity, and the alloy has high specific heat, resulting in reduced heat loss of liquid metal during mould filling.

Table 1: Typical nominal composition of SS304 (mass fraction in %) (D. Wang et al., 2018)

	C	Si	Mn	P	S	Cr	Ni	Mo	Cu	N	Fe
Stainless Steel 304	0.02	0.37	1.79	0.03	0.01	18.10	8.0	0.40	0.34	0.06	Balance

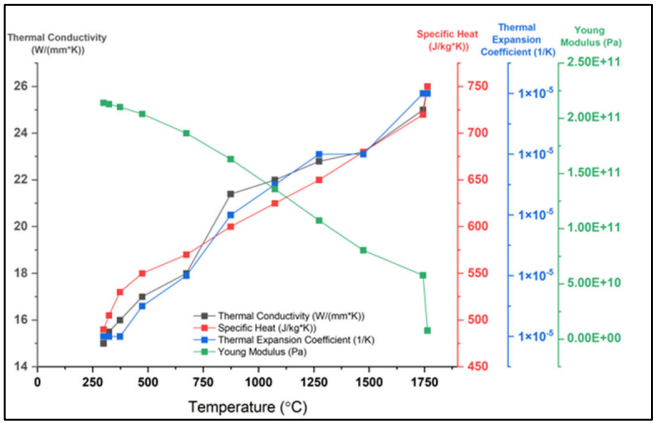

Figure 5: Thermophysical properties of the SS304 used in the numerical computation

Table 2: Thermal parameters of SS304 used in Altair Inspire Cast

Latent Heat (kJ/kg)	Liquidus Temperature (°C)	Solidus Temperature (°C)
270	1454	1399

2) Casting Design and Simulation Parameter

The gating system is responsible for sustaining the whole pattern and mould. It is a route for the alloy melt to produce the casting by directing the molten alloy into the mould. All cavities are filled in this way, directly influencing the casting quality and yield (Condruz and Badea, 2021). The gating system design alteration can reduce metal consumption per casting, which may affect industrial production economically (Šabík et al., 2021).

Four case studies were investigated to evaluate the effects of filling and solidification on the investment casting process and to identify strategies for mitigating flaws. The designs for the inlet, gating system, air vents, and casting components are specified in the Altair Inspire Cast. Figures 6(a)-(b) illustrate the casting design scheme proposals for case 1, divided into cases 1a and 1b, considering the effect of the solidification sequence in different orientations of the cast part of the vehicle barrier support. As seen in Figure 5(a), case 1a is intended to duplicate the actual casting process for the preliminary casting design in order to compare and evaluate shrinkage porosity. For case 1b, as seen in Figure 5(b), the casting component is optimized based on observing the final solidification region of liquid metal from the preliminary design, case 1a to mitigate shrinkage porosity.

To further optimize the investment casting process, Figure 6(c) shows a new casting design to improve the casting yield (case 2). The dimensions of the gating system used for case 1 in the numerical simulation are shown in Figure 7, in which the height of the gating system for case 1 and case 2 is decreased to half from case 1. Case 2 is divided into cases 2a and 2b to compare the influence of filling time for the new casting design which have better casting yield than casting design of case 1.

After assigning the material SS304 to the model, the casting's weight, density, and volume are computed and shown in Altair Inspire Cast. Cases 1a and 1b have the same casting parameters and weight since only the casting component is reoriented, but cases 2a and 2b have identical casting designs since the analysis observed the influence of the casting parameters. Case 1 and 2 are compared to its yield and weight, as shown in Table 3. The casting yield is calculated by dividing the weight of the casting part by the casting components' total weight. The differences in the casting parameters are shown in Table 3.

Table 3: Weight breakdown for Case 1 and Case 2

Weight Breakdown	Case 1	Case 2
Weight of both casting parts	5.3 kg	5.3 kg
Weight of gating system	1.7 kg	0.9 kg
Total weight of the casting / Total weight of metal poured	7.0 kg	6.1 kg
Casting yield	75.0 %	86.0 %

Table 4 shows the investment casting parameters used in the numerical study. The shell thickness is set at 10 mm, providing adequate support during the casting process while maintaining the desired shape and integrity of the final part. The shell mould material chosen is zircon sand, which is known for its high thermal stability, making it suitable for

high-temperature casting processes. Additionally, the initial shell temperature is maintained at 1000 °C, ensuring that the molten metal flows smoothly into the mould, reducing the risk of flaws such as cold shuts or misruns. These parameters are essential for ensuring the production of high-quality castings with minimal flaws. These parameters are set to be similar to the experimental setup. Table 5 illustrates the variations in filling time and pouring temperature, highlighting their impact on the occurrence of casting flaws.

Table 4: Investment casting process parameters

Casting Process Parameters	All Cases
Casting Material	Stainless Steel 304
Shell Thickness	10 mm
Shell Mould Material	Zircon Sand
Initial Shell Temperature	1000 °C

Table 5: Different of filling time and initial pouring temperature for these cases

Casting Process Parameters	Case 1 and 2a	Case 2b
Initial Pouring Temperature	1550 °C	1580 °C
Filling Time	20 seconds	10 seconds

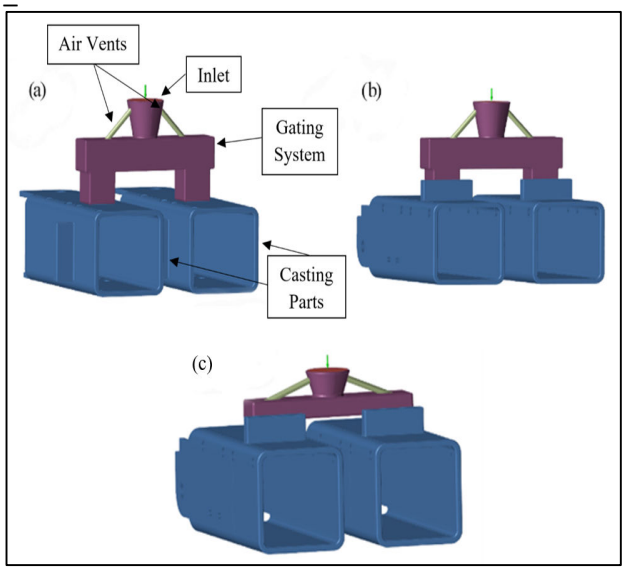

Figure 6: The two-gating system design, which consists of air vents, an inlet, a gating system, and casting parts for (a) Case 1a, (b) Case 1b and (c) Case 2

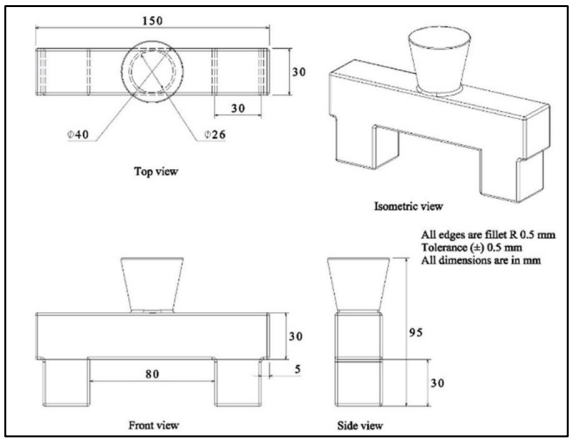

Figure 7: The runner of the casting

The accuracy of the casting process modelling significantly depends on the selection of boundary conditions and initial pouring temperature parameters for the material (D. Wang et al., 2018). Cases 1a and 1b used the same casting parameters. For cases 2a and 2b, two distinct filling time conditions, 10 and 20 seconds, are used to analyse filling-related flaws due to the smaller gating system.

The shell mould was heated to a temperature of 1000 °C with a thickness of 10 mm. Several studies have proven that the optimal preheating temperature for shell moulds in the investment casting process is 1000 °C (Carlson et al., 2002; Li et al., 2021). Zircon sand is used as the material for the shell mould. While the investment casting process consists of a shell and casting components, the simulation is simplified by merely modelling the cavities but ignoring the shell. The temperature-dependent material properties are obtained from the Altair Inspire Cast database. A total of 172,321 elements and 306,914 nodes were generated for the analysis of the simulation ensuring a detailed and accurate representation of the casting model.

III. RESULTS AND DISCUSSION

The most significant aspect of this study is the results and discussion section, which intends to compare the final result of the shrinkage porosity in the preliminary design between the case study and simulation. To ensure a reliable comparison, the studies were developed within similar casting process parameters. The results were separated into two cases in which cases 1a and 1b were compared to investigate the influence of the assembly of the casting components in mitigating shrinkage porosity. Cases 2a and 2b were analysed to improve the casting yield without flaws by comparing the casting parameters. The final modification, case 3, was proposed to be validated with an actual experiment due to industrial restrictions for fabricating the casting components.

A. Results of the numerical simulation

1) The influence of casting design on the investment casting solidification process

One of the many reasons the foundry uses simulation software is to predict the actual occurrence prevent potential flaws in production. Necessary adjustments can be made in the preliminary design process, which can help save high costs that would be otherwise used for fixing during production. Therefore, to validate the accuracy and reliability of this numerical model, it was necessary to analyse and compare shrinkage porosity results from the simulation results with the results retrieved from the actual casts. In Figure 8, the shrinkage porosity in the simulation results for case 1a was compared with the exact location of the visible shrinkage porosity. It is important to note that numerical simulation predicts where shrinkage porosity might occur in percentage, which means that it is possible to obtain slightly different results regarding the location and volume of the shrinkage porosity.

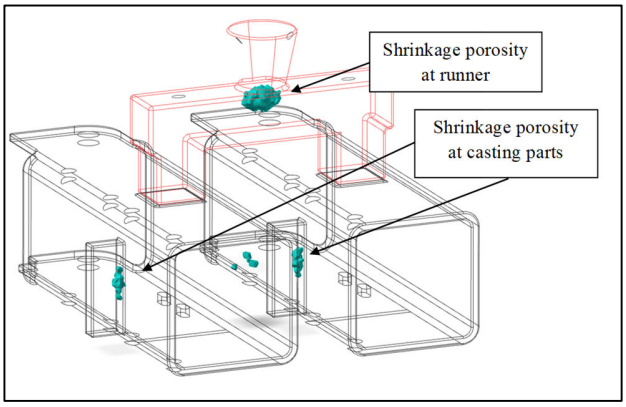

Figure 8: The location of shrinkage porosity at the casting part in the simulation result for case 1a

To explain why shrinkage porosity is observed for case 1a in the centre of the gating system and parts, the solidification process of the casting was analysed using the solid fraction result in Altair Inspire Cast shown in Figure 9. Shrinkage porosity is more likely to occur in a region where the casting section is isolated from the main feed, causing inadequate metal flow (Khalajzadeh and Beckermann, 2020). The solidification process starts from the edge of surfaces to the centre at 37 s. After 90 s of the solidification process, some areas of the casting part and gating system are still liquid. The actual location of shrinkage porosity (at 90 s) and centre of the gating system (at 442 s) in the casting component showed that the area was still in a liquid phase, but the surrounding area had solidified. This solidification path leads to the shrinkage of porosity during the casting process (Khalajzadeh and Beckermann, 2020).

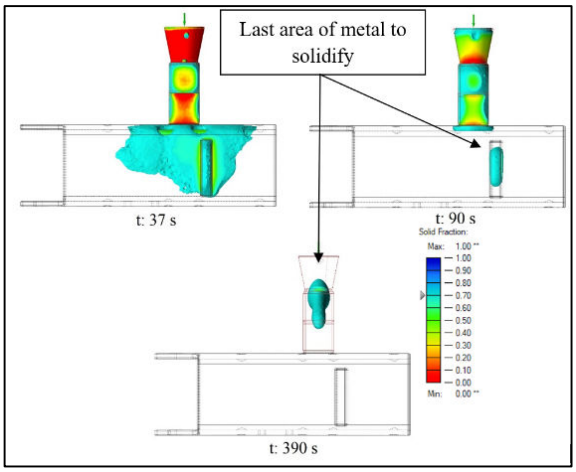

Figure 9:The location of shrinkage porosity at the casting part in the simulation result for case 1a

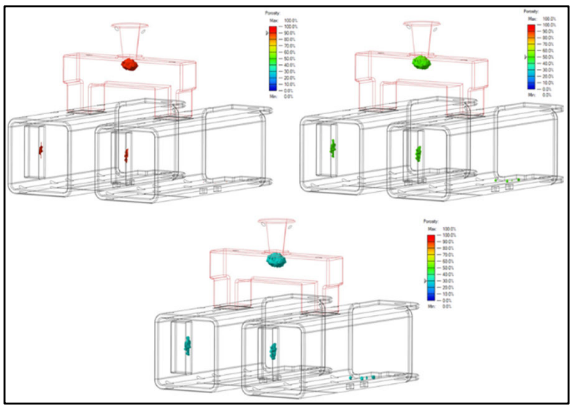

Figure 10: The size of shrinkage porosity (%) in casting parts for case 1a

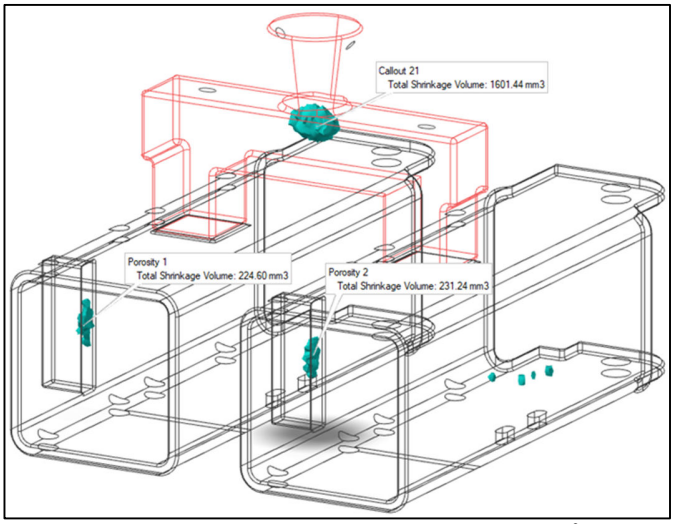

Figure 11: The result of total shrinkage volume (mm^3) for Case 1a

Figure 10 shows the porosity results, which visualize the areas of the ratio of voids to solid areas as more significant than or equal to the specified value. Changing the arrow at the legends, the shrinkage porosity can be analysed according to

the product's allowable range of shrinkage porosity. The higher percentage of porosity result shows a significant void occupied in the casting component in which the flaw occurred in a small area of the component. In comparison, the lower percentage of porosity implies several smaller voids and bigger voids that compensate for a more extensive area. In the case of the vehicle barrier support, the shrinkage porosity is not acceptable in which the pores occurred, which can lead to structural integrity of the component. To mitigate the flaw, the casting design should promote directional solidification of the metal ensuring the isolated section solidified last by allowing the molten metal to continuously feed. Figure 11 shows a total of 455 mm3 of shrinkage volume was measured at the porosity location which indicates a complete void at the particular area which aligns with the findings from the experimental study.

By reorienting 90 degrees of the casting product relative to the gating system, the new casting design, case 1b, was developed in Figure 12. The solid fraction result showed that the metal last solidified at the centre of the runner (t = 460 s). At the previously isolated area where shrinkage porosity was observed, during t = 125 s, the results showed that the section of the casting was not separated from primary molten metal and still fed the liquid to the area. Thus, the intended location is not the last region for metal to solidify.

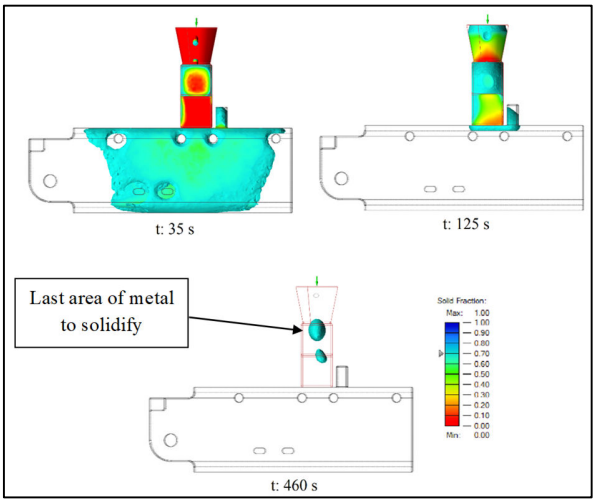

Figure 12: Solidification of the melt for case 1b over a period of time

Figure 13 shows the porosity results for case 1b. It is observed that a proportion of 30 % porosity occurred at the body of the casting part in case 1b. By strategically orienting 90 degrees of the vehicle barrier support to the vertical axis, the casting design in this case eliminate the shrinkage porosity at isolated section, allowing compensation of volume shrinkage during the solidification. As in the actual investment casting process, the substantial amount of porosity in the gating system will be disregarded. The cast of the gating system will be cut off and remelted to create a new casting product (Rajaram et al., 2024). From these results, cases 2 were developed to produce better investment casting yield. Figure 14 shows the result of shrinkage porosity shown no occurrence of shrinkage flaw. However, another flaw was occurrence in this study which related to the pouring time.

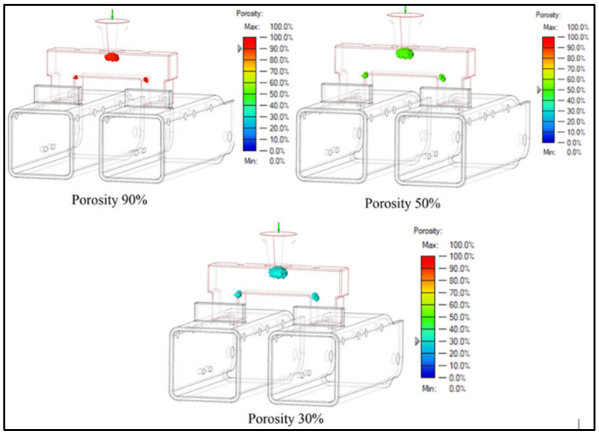

Figure 13: The size of shrinkage porosity (%) in casting parts for case 1b

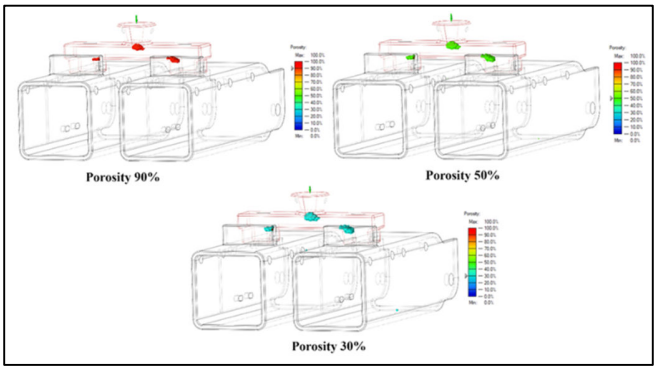

Figure 14: The size of shrinkage porosity (%) in casting parts for both case 2a and 2b

2) The influence of filling time on the investment casting solidification process

A further optimization of the casting design from case 1b, case 2a has been developed to enhance casting yield by utilizing the simulation software. By reducing the runner's height by half, material usage in the gating system can be significantly minimized. However, adjustments to the casting design without considering the process parameters in the investment casting process can lead to the occurrence of flaws. The result showed that the runner in gating system is crucial in controlling the flow of molten metal into the mould which substantially affects the quality and functionality of the casting (Hao et al., 2022). Figure 15 illustrates that two different filling times were applied to finish the filling process with varying designs of casting. In case 2b, the filling period for completed casting is 10 seconds, while cases 1a, 1b, and 2a require 20 seconds for molten metal to fill the cavity completely.

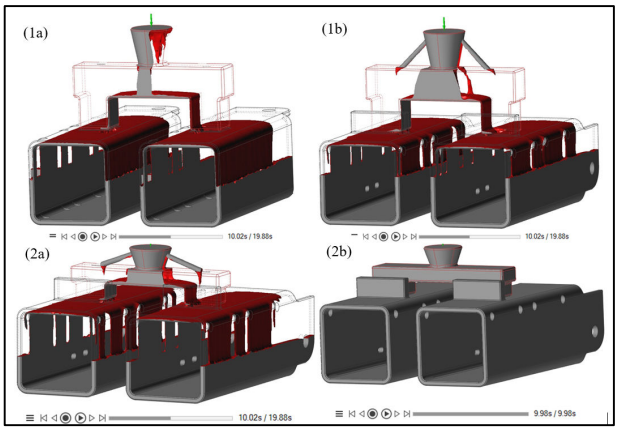

Figure 15: Filling of molten metal for cases 1a, 1b, 2a, and 2b, within 10 seconds, respectively

In Altair Inspire Cast, the red contour regions in Figure 15 shows where two material fronts meet with a high-temperature differential between the melt where the cold shut is present in case 2a. Casting in near-solidus temperature also is likely prone to cold shut because the metal is solidified prematurely before the casting is complete (Borikar et al., 2017). In the simulation, the following equation was used to predict cold shuts in Kelvin (K):

$$\Delta T = T_{inlet} - \frac{(T_{front1} + T_{front2})}{2} \quad (1)$$

where,

- ΔT is the values of the legend are derived by subtracting the average temperature of the fronts.
- T_{front1} and T_{front2} are temperatures measured at two different points along the front of the casting.
- T_{inlet} is the inlet temperature.

Cases 2a and 2b in Figure 16(a)-(b) show a filling-related casting flaw, cold shuts. Case 2a was made under the same filling time as case 1. The analysis showed that case 2a had severed cold shut compared to case 2b. When the filling time was made the same as the parameters from the previous design, it can lead to premature freezing of the melt during the filling process because of the reduced flow rate. By reducing the filling time to complete the casting process in case 2b, the results show that the parameters used mitigated the flaws completely.

The optimal shell thickness and pouring temperature are crucial factor for ensuring high-quality castings (Raza et al., 2015). However, it is not solely determined the occurrence of flaws. Instead, it is also depending on a balance between slow and high filling time which longer filling time can lead to cold shuts, and fast filling will take the onset of surface instability. Thus, a filling time of 10 seconds in case 2b was the optimized casting design for eliminating the cold shut.

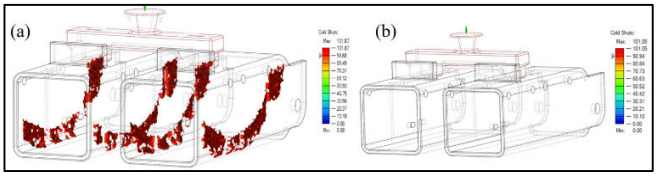

Figure 16: Comparison of cold shuts flaws between (a) case 2a and (b) case 2b

B. Experimental Validation

Following the comprehensive numerical computation of the investment casting process where the shrinkage porosity has been predicted and optimized. Due to industrial restrictions to develop the optimized runner, the new gating layout was implemented. Figure 17 shows the modification of the case 1b casting design, which is the development of the stainless-steel vehicle barrier support and the actual shell mould named Case 3 manufactured by the foundry. The assembly of the gating system is repositioned according to technical expertise in which the initial assembly was challenging during removing the cast product from the gating system after the complete casting.

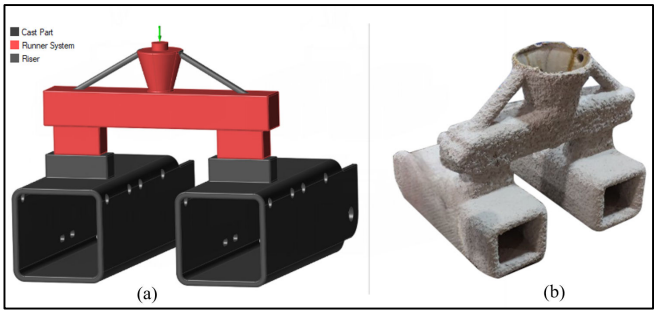

Figure 17: (a) The CAD model and (b) the actual casting component of the optimized casting design fabricated

Therefore, from the simulation results in Figure 18, the previous location where the shrinkage porosity occurs is utterly mitigated. There are several porosities was observed with arrows at one the casted components. However, it was observed that the measured of shrinkage volume was below than 15mm^3 which not visualized by the software compared to the shrinkage at the runner which shown in Figure 19. The optimized gating position allows the molten metal to have a good solidification path and sequence during the solidification stage, as in case 1.

The actual casting part is fabricated as shown in Figure 20 to validate the simulation results. The porosity results showed good agreement between simulation and experiment in predicting the shrinkage porosity. Thus, from this study, the demonstration of casting simulation software allows the foundry to forecast the flaws in the early phase of casting development before entering production, which could cause higher correction costs.

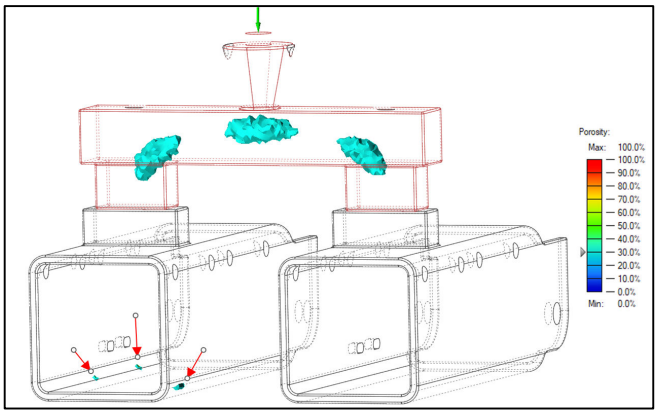

Figure 18: The simulation result of shrinkage porosity shows that the previous location of porosity has been eliminated

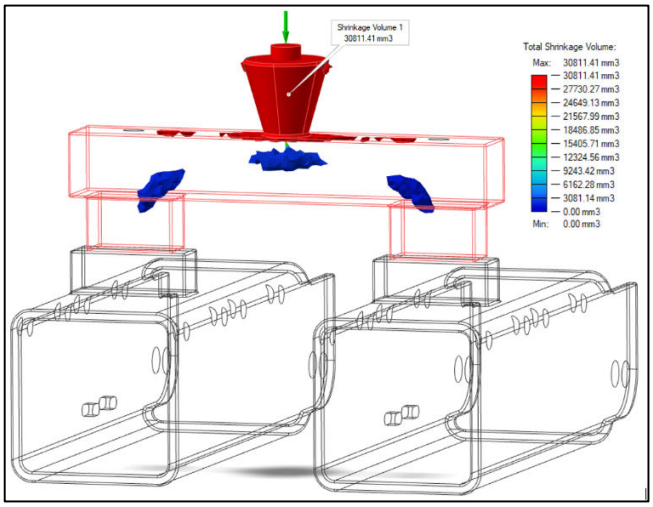

Figure 19: The result of the total shrinkage volume for Case 3

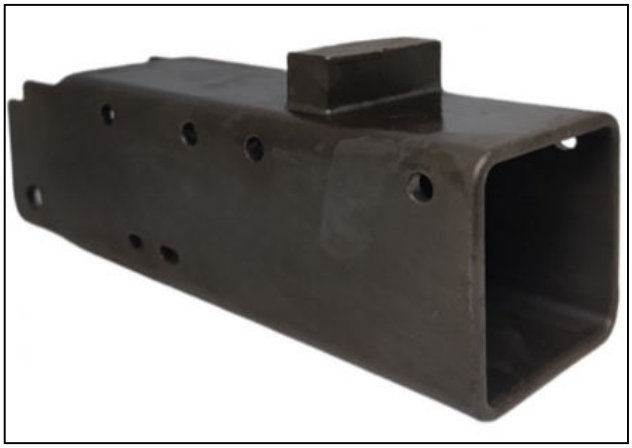

Figure 20: The actual casting product shows that casting simulation is successful in giving insight into predicting and preventing the occurrence of flaws

IV. CONCLUSION

The primary goal of this research was to eliminate the occurrence of shrinkage porosity through the application of numerical simulations, subsequently validated via experimental procedures. In the investment casting process, the casting designs and filling time play significant roles in determining the final quality of the casting. The occurrence of porosity is due to improper casting design which can lead to reduced mechanical properties. By repositioning the casting design of the vehicle barrier support with the gating system, the potential flaws can be reduced ensuring a more efficient solidification path. On the other hand, the filling time influences the uniformity of the material flow during the casting process affecting the formation of cold shut. Implementing a 50% reduction in the runner's height with pouring time of 10 seconds, the casting design resulted in a 10% improvement in casting yield without the occurrence of cold shut. Due to industrial constraints, final modifications were made to the casting design to verify the simulation results with the actual product fabrication in the foundry. The result of the actual fabrication shows good agreement with simulation, demonstrating a significant stride towards achieving a flaw-free product.

AUTHOR CONTRIBUTIONS

Mat, M. F.: review and supervision. **Rahman, A. R. A.:** Writing- original draft. **Manurung. Y. H. P.:** Supervision-review and editing. **Adenan, M. S.:** Methodology. **Sigeregar. I.:** Formal analysis and Funding acquisition. **Kasim, K.:** Conceptual Analysis. **Kung, T. C.:** Experimental testing **Syafiq, A.:** Software technical **Busari, Y. O.:** Theoretical Framework

REFERENCES

Ahmad, S. N., Manurung, Y. H., Adenan, M. S., Yusof, F., Mat, M. F., Prajadhiana, K. P., Minggu, Z., Leitner, M., & Saidin, S. (2022). Experimental validation of numerical simulation on deformation behaviour induced by wire arc additive manufacturing with feedstock SS316L on substrate S235. *International Journal of Advanced Manufacturing Technology*, *119*(3–4), 1951–1964.

Borikar, V. N., Kapgate, P. G., Wairagade, R. A., & Kshirsagar, A. D. (2017). *Optimization of Casting Components by Minimizing Cold Shut Defect*. *5*(3), 3–5.

Bruna, M., Bolibruchová, D., Pastirčák, R., & Remišová, A. (2019). Gating System Design Optimization for Investment Casting Process. *Journal of Materials Engineering and Performance*, *28*(7), 3887–3893.

Carlson, K. D., Ou, S., Hardin, R. A., & Beckermann, C (2002). Development of new feeding-distance rules using casting simulation: Part I. Methodology. *Metallurgical and Materials Transactions B: Process Metallurgy and Materials Processing Science*, *33*(5), 731–740.

Choe, C. M., Yang, W. C., Kim, U. H., Ri, B. G., & Om, M. S. (2022). Manufacture of centrifugal compressor impeller using FDM and investment casting. *International Journal of Advanced Manufacturing Technology*, *118*(1–2), 173–181.

Condruz, M. R., & Badea, T. A. (2021). *Computational And Experimental Study on Defect Emergence in Computational and Experimental Study on Defect Emergence In Investment Cast*. *January*.

Feng, Y., Liao, D., & Chen, T. (2021). *Confluence And Cold Shut Computation Based on Time Field in Casting*

Simulation. *18*(2), 101–109.

Fu, M. W., & Yong, M. S. (2009). Simulation-Enabled Casting Product Defect Prediction in Die Casting Process. *International Journal of Production Research*, *47*(18), 5203–5216.

Hao, X., Liu, G. Huai, Wang, Y., Wu, S. Ping, & Wang, Z. Dong. (2022). Optimization Of Investment Casting Process for K477 Superalloy Aero-Engine Turbine Nozzle by Simulation and Experiment. *China Foundry*, *19*(4), 351–358.

Jadhav, R., & Mane, V. (2020). *Design And Analysis of Gating System at Various Orientation for Rear Break Drum By Using Casting Simulation Software*. *2*.

Jones, C. A., Jolly, M. R., Jarfors, A. E. W., Irwin, M., Svenningsson, R., Steggo, J., & Eriksson, J. (2020). A Verification of Thermophysical Properties of a Porous Ceramic Investment Casting Mould Using Commercial Computational Fluid Dynamics Software. *Iop Conference Series: Materials Science and Engineering*, *861*(1).

Khalajzadeh, V., & Beckermann, C. (2020). Simulation Of Shrinkage Porosity Formation During Alloy Solidification. *Metallurgical And Materials Transactions A: Physical Metallurgy and Materials Science*, *51*(5), 2239–2254.

Khan, M. A. A., & Sheikh, A. K. (2018). A Comparative Study of Simulation Software for Modelling Metal Casting Processes. *International Journal of Simulation Modelling*, *17*(2), 197–209.

Kumar, V., Ali, B., & Khan, N. (2018). Analysis Casting Simulation and Its Importance. *Iosr Journal of Engineering (Iosrjen)*, *08*(6), 72–82. Www.Iosrjen.Org

Kuo, J. K., Huang, P. H., Lai, H. Y., & Chen, J. R. (2017). Optimal Gating System Design for Investment Casting Of 17-4ph Stainless Steel Enclosed Impeller by Numerical Simulation and Experimental Verification. *International Journal of Advanced Manufacturing Technology*, *92*(1–4), 1093–1103.

Li, F., Wang, Y., Wang, D., & Zhao, Y. (2021). *Comparison Of Various Gating Systems for Investment Casting of Hydraulic Retarder Impeller with Complex Geometry*. *235*(4), 583–593

Liu, Y., He, H., Gao, J., Li, G., Liang, Y., & Li, L. (2022). Research on the Low-Pressure Casting Process of a Double Suction Impeller In 304 Austenitic Stainless Steel with High Performance and Thin-Wall Complex Structure. *Journal Of Physics: Conference Series*, *2390*(1).

Malik, I., Sani, A. A., & Medi, A. (2020). Study On Using Casting Simulation Software for Design and Analysis of Riser Shapes in A Solidifying Casting Component. *Journal Of Physics: Conference Series*, *1500*(1).

Mat, M. F., Manurung, Y. H. P., Muhammad, N., Ditler, A., Abd Ghani, M. S., & Leitner, M. (2020). Grain Growth Prediction of Bead-On-Plate with Filler Wire Ss316l Using Fem. *Iop Conference Series: Materials Science and Engineering*, *834*(1).

Precision Forming Technology of Large Superalloy Castings for Aircraft Engines. (N.D.).

Rafique, M. M. A., & Iqbal, J. (2009). Modeling And Simulation of Heat Transfer Phenomena During Investment Casting. *International Journal of Heat and Mass Transfer*, *52*(7–8), 2132–2139.

Rajaram, D., Sooriyamoorthy, E., & Sankaranarayanan, A. K. (2024). Automated Optimization of Gating System Through Numerical Simulation. *Proceedings of the Institution of Mechanical Engineers, Part B: Journal of Engineering Manufacture*.

Raza, M., Irwin, M., & Fagerström, B. (2015). The Effect of Shell Thickness, Insulation and Casting Temperature on Defects Formation During Investment Casting of Ni-Base Turbine Blades. *Archives of Foundry Engineering*, *15*(4), 115–123.

Šabík, V., Futáš, P., Pribulová, A., & Delimanová, P. (2021). *Optimization of a Gating System by Means of Simulation Software to Eliminate Cold Shut Defects In Casting*. *5*(1), 1–4.

Wang, D., Dong, A., Zhu, G., Shu, D., Sun, J., Li, F., & Sun, B. (2018). *Rapid Casting of Complex Impeller Based On 3d Printing Wax Pattern and Simulation Optimization*.

Wang, X., & Zhang, Z. (2011). *Simulation Of Flow Field and Temperature Tieldi in The Process Of Filling And Solidification For K424 Alloy Thin-Walled Casting*. *68*, 1568–1573.